NASA Technical Memorandum 79281

DYNAMIC RESPONSE OF DAMAGED ANGLEPLIED FIBER COMPOSITES

C. C. Chamis, J. H. Sinclair
and R. F. Lark
Lewis Research Center
Cleveland, Ohio

Prepared for the
Winter Annual Meeting of the
American Society of Mechanical Engineers
New York, New York, December 2-7, 1979

DYNAMIC RESPONSE OF DAMAGED ANGLEPLIED FIBER COMPOSITES

C. C. Chamis, J. H. Sinclair and R. F. Lark

NASA-Lewis Research Center
Cleveland, Ohio 44135

ABSTRACT

An investigation was conducted to determine the effects of low level damage induced by monotonic load, cyclic load and/or residual stresses on the vibration frequencies and damping factors of fiber composite angleplied laminates. Two different composite systems were studied - low modulus fiber and ultra high modulus fiber composites. The results obtained showed that the frequencies and damping factors of angleplied laminates made from low modulus fiber composites are sensitive to low level damage while those made from ultra high modulus composites are not. Also vibration tests may not be sufficiently sensitive to assess concentrated local damage in angleplied laminates. And furthermore, dynamic response determined from low-velocity impact coupled with the Fast Fourier Transform and packaged in a minicomputer can be a convenient procedure for assessing low-level damage in fiber composite angleplied laminates.

INTRODUCTION

A major concern in the fiber composites community has been the static and dynamic response of slightly damaged (not visually discernable) angleplied fiber composites. Coupled with this concern is the need to use a convenient mechanical test to identify both the effects and the extent of damage. In response to this concern and need, an investigation was conducted at Lewis Research Center (LeRC) with the primary objective to assess the dynamic response of slightly damaged angleplied laminates. A secondary objective of the investigation was to identify a convenient dynamic test that can be used to assess this damage. The investigation was both experimental and theoretical in nature.

In the experimental part, angleplied laminates $[\pm 45, 90_2, 0_2]_S$, (quasi-isotropic) were made from two composite systems. One system was E-glass fiber/epoxy matrix (E-G/E) and the other was ultra high modulus graphite fiber/epoxy matrix (T-75/E). These combinations of laminate configuration and composite system were selected to bound the magnitudes of elongation to fracture

and the magnitudes of lamination residual stresses. Specimens from these laminates were subjected to cyclic mechanical load tests until a change in the stress-strain curve was observed. Specimens were also loaded monotonically to fracture. After these tests, segments from the specimens were subjected to low level impact tests. Their dynamic response (frequencies and damping factors) were determined using the Fast Fourier Transform Method available in a minicomputer. The specimens tested were ultrasonically C-scanned prior to and after the cyclic testing.

In the theoretical portion of this study, laminate analysis was used to determine first ply failures including both lamination residual stresses and those due to mechanical load. NASTRAN was used to determine the vibration frequencies of the specimens simulating the test conditions. The mechanical properties required by NASTRAN for both undamaged and damaged specimens were generated using laminate theory.

EXPERIMENTAL

The experimental part of the investigation consisted of fabricating, instrumenting, and testing the specimens.

Laminate Fabrication

The laminates were made at the Lewis Research Center using commercial Thornel-75 graphite/PR288 (T-75/E) and E-glass/1003 (E-G/E) prepregs. Individual plies of prepreg were stacked at the required fiber orientations in metal molds to form the 12 ply angleplied laminates. A thermocouple was inserted into one end of each uncured laminate. For the T-75/E laminate the cold mold was placed in a hydraulic press the platens of which had been heated to 450 K (350° F). A contact pressure of 0.10 MPa (15 psi) was applied on the mold. This pressure was maintained for 3 minutes after the laminate reached 311 K (100° F); then the pressure was increased gradually over a 2 minute period to 2.1 MPa (300 psi). This pressure was maintained for 2 hours after which the mold containing the cured composite was taken from the press. The laminate was then removed and allowed to cool to room temperature. For the E-G/E laminate, the press platens were preheated to 436 K (325° F). The cold mold was placed in the press and contact pressure was applied and maintained for 3 additional minutes after the thermocouple indicated 311 K (100° F). Then the pressure was increased gradually over a period of 2.5 minutes to 0.34 MPa (50 psi). Press temperature and pressure were then held constant for an hour at which time the power was turned off and the laminate allowed to cool under pressure. The laminate was postcured in the mold under a weight of 4.54 kg (10 lb) for 16 hours at 411 K (280° F).

Specimen Preparation, Instrumentation, and Testing

The laminates were cut into test specimens 2.54 cm (1-in.) wide using a diamond cutting wheel. Specimen length was 30.5 cm (12-in.). Specimen ends were reinforced with 5.1 cm (2-in.) long adhesively bonded fiberglass end tabs leaving gage lengths of 20 cm (8-in.). Each tensile specimen was instrumented with one 120-ohm, 90° delta rosette strain gage located at midlength for specimens that were to be tested monotonically to fracture. So as not to interfere with subsequent frequency testing, the gages were located at about 1.2 cm (0.5 in.) from one end of the test section on the specimens that were to have damage induced via cyclic loading.

A specimen of each material was loaded to fracture in a hydraulically actuated universal testing machine. Testing was in-

cremental to facilitate periodic recording of strain gage data. Stress-strain curves were also plotted concurrently with the testing to observe changes in slope of these curves that might indicate damage. Based on information obtained from the destructive testing of these two specimens, other specimens were subjected to cyclic loading at stresses large enough to induce damage but not sufficiently large to cause fracture. Damage thus achieved was revealed by ultrasonic C-scans of specimens treated as described above. Specimens 10.2 cm (4-in.) long were taken from selected areas of these tested tensile specimens and from untested material for determination of vibration frequencies and damping factors via low velocity impact excitation tests.

Measurement of Frequencies and Damping Factors

The vibration frequencies and the damping factors were determined by a special procedure which was developed at the University of Cincinnati under contract to NASA Lewis Research Center. The tests and data reduction were conducted at the University of Cincinnati as a part of this same contract. In this procedure the test specimen is considered to be a free beam. Briefly, then, the procedure is as follows. The beam, suspended vertically by means of low mass silk threads bonded to the beam edge, was excited with an impact from a small ball bearing and the response was measured with a wide-frequency response microphone. There were no transducers in contact with the beam. There was no measurable loading of the beam. A zoom transform was used with a LaPlace transform algorithm (Fast Fourier Transform) to compute both the natural frequency and damping factor. The beam was tested with a number of identical impacts at different times. The measurements were reproducible within a maximum standard deviation of 0.0013 percent for natural frequencies and 1.3 percent for modulus of elasticity. This error, of course, can be reduced by averaging a number of impacts by a $1/\sqrt{n}$ factor.

The zoom transform was used to achieve a small delta frequency and the LaPlace transform was used to compute the natural frequencies from the zoomed data.

Since the beam was small, it was not practical to mount a transducer on the beam. Therefore, the mode shape information was determined by mounting a small known mass on the beam and measuring the change in natural frequency due to the mass. The change in the natural frequency can be used to compute the effective mass of the beam's modes of vibration at the point where the mass has been added. By moving the mass over the surface of the beam, the mode shape can be measured.

The effective mass of the mode of vibration can be determined by the following relationship:

$$M_e = \frac{M_a}{\frac{\omega_i^2}{\omega_a^2} - 1}$$

where M_e = effective mass
M_a = added mass
ω_i = initial natural frequency
ω_a = natural frequency with added mass

THEORETICAL PART

The theoretical part of the investigation consisted of laminate analysis and finite element analysis via NASTRAN.

Laminate Analysis

Laminate analysis was used to predict the laminate moduli, ply residual stresses, ply stresses at fracture and the material properties needed for input to NASTRAN. The actual calculations were performed using the composite mechanics computer code[1]. The damage induced in the laminate by the residual stresses, the preloading and the cyclic loading was simulated indirectly using an equivalent void volume ratio in the computer code. In essence this approach considers the laminate to have uniform damage distribution which is acceptable for frequency calculations but not for local stresses. In addition the effects of possible shear coupling were simulated by permitting the laminate to be slightly anisotropic in its plane.

Finite Element Analysis

The finite element analyses were performed to predict the free-beam vibration frequencies of the specimens and the effects of low level damage, due to factors mentioned previously, on these frequencies. Additional analyses were performed to assess the effects on the frequencies of through-the-thickness defects in the middle of the specimen. The finite element model of the specimen that was used in NASTRAN[2] is shown in Figure 1. It consists of 297 nodes, 256 quadrilateral anisotropic plate (CQUAD2) elements, and 1485 degrees of freedom (DOF). This type of model was considered reasonable to simulate the effects of low level damage on the free vibration response of these specimens. The through-the-thickness defects were simulated by removing two elements (124 and 125) from the center of the specimen.

RESULTS, COMPARISONS AND DISCUSSION

The experimental and predicted results obtained in this investigation for the various properties described previously are summarized, compared and discussed in this section. Comparisons between experimental and predicted results are also summarized.

Stress-Strain Curves

Typical monotonic and cyclic stress-strain curves of the specimens tested are shown in Figure 2. These curves indicate changes in the initial and tangent slopes for both the E-G/E and the T-75/E composites under both monotonic and cyclic loading. This indicates that both loadings have induced damage in the specimens. Note also the "apparent hysteresis" in the cyclic loading curves. The corresponding Poisson's strain curves are shown in Figure 3. As can be seen in this figure, the Poisson's strain curves show similar behavior as the stress-strain curves. C-scan traces for the specimens are shown in Figure 4. These traces show considerably more damage for the T-75/E composite specimens than for the E-G/E specimens. Photographs of typical specimens tested including some of those tested to fracture, are shown in Figure 5.

Ply Stresses

Unidirectional and angleplied composite properties of the specimens required for the various analyses were predicted using the computer code[1]. These properties are summarized in table I. Limited available experimental data for these specimens are also shown for comparison.

As can be seen the predicted values are in good agreement with the available experimental data (within 10 percent for moduli).

The calculated transverse residual stresses in a given ply of the angleplied laminates were 25 MPa (3.6 ksi) for the E-G/E and 33 MPa (4.8 ksi) for the T-75/E. The corresponding longitudinal stresses have the same magnitude but opposite sign, while the intralaminar shear stresses are "zero". These types of residual stress states are characteristic in quasi-isotropic angleplied laminates.

Calculated ply stresses at fracture loads, obtained using the properties shown in table I and including residual stresses, are summarized in table II. The combined-stress failure-criterion values for the plies are given in the column "Margin-of-Safety" (MOS). Negative values in this column indicate ply failure. Typical uniaxial ply strengths (fracture stresses) are also given in this table. Based on the negative MOS values, the $\pm$ plies and the 90° plies failed in both the E-G/E and the T-75/E laminates. Comparing ply stresses with the corresponding ply strengths, it is seen that the $\pm$45° and 90° plies failed in transverse tension. About one-fourth of the transverse ply stress in the E-G/E laminate is due to residual stress as is about 80 percent in the T-75/E laminate. It is worth noting that the ply transverse residual stresses in the T-75/E laminates 33 MPa ((4.8 ksi)) are greater than the corresponding ply strength (29 MPa (4.0 ksi)) and cause transply cracks in the laminate as shown in Figure 6. The transverse ply stresses, at the cyclic stress shown in the ultrasonic C-scan (fig. 4c), are respectively: 85 MPa (12.3 ksi) in the $\pm$45° plies of the E-G/E laminate and 41 MPa (6.0 ksi) in the $\pm$45° plies of the T-75/E. Both of these are greater than the corresponding transverse ply strengths in Table IIb and, therefore, induce damage (transply cracks) in these laminates. The corresponding transverse ply stresses in the 90° plies are about twice as large and the damage will be more severe in these plies. Recall that the magnitude of the cyclic stress was selected based on the changes in the slope of the stress-strain curves shown in Figure 2. The calculated ply stresses just described show which ply stresses induce the damage.

The above discussion demonstrates directly and indirectly that the cyclic load used in the investigation induced damage in the 0°, $\pm$45°, and 90° plies in both E-G/E and T-75/E laminates.

Vibration Modes and Damping Factors

The measured results, obtained from the special procedure described previously, for free vibration frequencies and damping factors were determined from frequency response spectrums such as those shown in Figure 7. The reduced data are summarized in Table III. Note the results shown are normalized with respect to those for the undamaged specimens for ease of comparison.

It can be seen in Table III that the frequency decreases with increased load (damage) for the E-G/E laminates as was expected. The decreases in frequency range from about 3 percent to 6 percent. The damping factor increases ranging from about 1 percent to about 29 percent for the lower load case and from about 3 percent to 18 percent for the higher load case. An exception to this is the damping factor for the second frequency which decreases for the lower load case and increases for the higher load case. This indicates some kind of an anomaly that may be attributed, in part, to the degree of coupling between bending and torsion. The conclusions to be drawn from these results are:

1. The frequency of E-G/E laminates decreases in the presence of damage although this decrease may be small and may be shadowed by the effects of other factors; and (2) the damping factor for E-G/E laminates increases in general with no clear correlation between

damping and damage.

The results for the T-75/E laminates in Table III show progressive increases in frequencies with increased load (damage) and a mixture of increases and decreases for damping. These may be caused, in part, by the high stiffness which minimizes the vibration amplitudes. The conclusion from these results is that frequencies or damping factor may not be sensitive discriminators for damage assessment in T-75/E laminates.

The experimentally determined frequencies and those predicted using NASTRAN are summarized in table IV for comparison. The following points are worthy of note. For the E-G/E laminate:

1. Two more frequencies were predicted than were determined by measurement;
2. The predicted frequencies are in good agreement with the corresponding measured ones (within 5-percent) for the undamaged case (compare column 1 with column 5);
3. Twenty percent void equivalent in all the elements was needed to simulate the damage induced by the loads (column 8);
4. Simulation using shear coupling (column 6) and damage in selected regions in the specimen (column 7), based on the C-scans (fig. 4c), is not sensitive enough to predict the measured reduction in frequencies (column 2 or 3);
5. The free frequencies are insensitive to local damage (through-the-thickness defect at the specimen center, with defect-length/specimen width equal to 1/4), (column 9).

For the T-75/E laminate:

1. Three frequencies were determined by measurement which were not predicted using NASTRAN and two frequencies were predicted which were not determined by measurement.
2. The predicted frequencies are within about 3 percent of the corresponding measured ones for the undamaged specimens (compare columns 1 with 5);
3. The measured frequencies are not sensitive to load and residual stress damage as was already mentioned in the previous section;
4. Shear coupling and partial damage have negligible effects on the predicted frequencies (less than 2 percent, columns 6 and 7);
5. A uniform damage simulated by 20 percent voids in all the elements reduces the predicted frequencies by about 11 percent (column 8);
6. Concentrated local damage has negligible effect on the free vibration frequencies (column 9).

It is apparent from the above discussion that both experimental and analytical methods may be needed to determine the various modes in a vibration analysis. It is also apparent that the experimental procedure described herein, low-velocity impact coupled with the Fast-Fourier Transform and packaged in a mini-computer, can be a convenient procedure for assessing low-level damage on the dynamic response of fiber composite angleplied laminates.

The first five vibration mode shapes corresponding to the vibration frequencies column 9, Table IV are shown in Figure 8. As can be seen in this figure the mode shapes are primarily bending and torsion. It is noted that frequencies for the first, second and third bending modes are not integer multiples of each other. Neither are the two torsional frequencies. This means that each of the mode shapes in Figure 8 has some degree of coupling between bending and torsion. Typical mode shapes plotted from the data obtained from the experimental procedure are shown in Figure 9 for the first and second bending modes. As can be seen by inspection these modes are in excellent qualitative agreement with the corresponding predicted ones in Figure 8.

CONCLUSIONS

The major conclusions of an investigation to assess the sensitivity of the dynamic response (free vibration frequencies and damping factors) of fiber composite angleplied laminates to low-level damage induced by load (monotonic and cyclic) and residual stress are as follows:

1. Monotonic load, cyclic load and/or residual stress induced damage may reduce the free vibration frequencies and may increase the damping factor in low modulus fiber composites such as E-Glass/Epoxy (E-G/E) angleplied laminates, while it may have negligible effect, if any, in ultra high modulus fiber composites such as Thornel-75/Epoxy (T-75/E) angleplied laminates.
2. Proper simulation of load induced damage for analysis may require considerable judgment and intuition.
3. Free vibration tests may not be sufficiently sensitive to assess concentrated local damage in angleplied composite laminates.
4. Both experimental and analytical methods may be needed to determine the various modes in vibration analyses.
5. Dynamic response determined from low-velocity impact coupled with the Fast-Fourier-Transform and packaged in a minicomputer can be a convenient procedure for assessing low-level damage in fiber composite angleplied laminates.

REFERENCES

1. Chamis, C. C., "Computer Code for the Analysis of Multilayered Fiber Composites - Users Manual," NASA TN D-7013, 1971.

2. McCormick, C. W., ed., "NASTRAN Users Manual (Level 15), NASA SP-222 (01), 1972.

TABLE I. - SUMMARY OF UNIDIRECTIONAL AND ANGLE-PLIED LAMINATE PROPERTIES

Property	Unidirectional composite				Angle-plied laminate			
	E-glass/epoxy		T-75/epoxy		E-glass/epoxy		T-75/epoxy	
	Predicted	Measured	Predicted	Measured	Predicted	Measured	Predicted	Measured
Longitudinal modulus[a], 10^6 psi	6.96	6.3	38.0	35.3	3.48	[c]3.4	16.1	16
Transverse modulus[b], 10^6 psi	1.70		.83	.83	3.48		16.1	
Shear modulus, 10^6 psi	.82		.49		1.13		3.61	
Major Poisson's ratio	.25	.29	.24	.32	.30	.25	.30	.2[c]
Longitudinal temperature expansion coefficient (10^{-6} in./in. ^oF)	3.88		-.31		6.30		.30	
Transverse temperature expansion coefficient (10^{-6} in./in. ^oF)	14.0		19.6		6.30		.30	

[a]Along fiber direction for unidirectional composite; along zero ply direction for angleplied laminates.

[b]Transverse to fiber direction for unidirectional composite; transverse to zero ply direction for angleplied laminates.

[c]Fitted slope.

Conversion factors: 10^6 psi = 6.8947 GPa
$^oF^{-1} \times 1.8 = K^{-1}$

TABLE II. - CALCULATED PLY STRESSES AT FRACTURE, INCLUDING RESIDUAL STRESSES, AND CORRESPONDING UNIAXIAL PLY STRENGTHS

(a) Ply stresses

Composite	Fracture strength, ksi	Ply stresses, ksi											
		±45° Plies				90° Plies				0° Plies			
		Longitudinal	Transverse	Shear	[a]Margin of safety	Longitudinal	Transverse	Shear	[a]Margin of safety	Longitudinal	Transverse	Shear	[a]Margin of safety
E-glass/epoxy	59.6	41.3	18.3	-16.9	-.38	-17.9	31.7	0	-.63	100	5.0	0	-0.36
T-75/epoxy	44.8	38.8	6.0	1.6	-.53	-25.7	7.0	0	-2.7	103	4.9	0	.67

(b) Uniaxial ply strengths

Composite	Uniaxial ply strength, ksi				
	Longitudinal tensile	Longitudinal compressive	Transverse tensile	Transverse compressive	In-plane shear
E-glass/epoxy	170	97	4	17	5
T-75/epoxy	142	126	4	19.8	7.1

[a]Combined stress failure.

Conversion factor: GPa = ksi × 0.68947×10^{-2}

TABLE III. - NORMALIZED FREQUENCIES AND DAMPING FACTORS (EXPERIMENTAL)

Composite	Vibrational mode	Frequency				Damping factor				
		Undamaged	After loading to			Undamaged	After loading to			
			0.193 GPa (28.2 ksi)	0.333 GPa (48.3 ksi)			0.193 GPa (28.2 ksi)	0.333 GPa (48.3 ksi)		
E-glass/epoxy	1	1.000	0.941	0.941		1.000	1.276	1.125		
	2	1.000	.978	1.00		1.000	.637	.765		
	3	-----	-----	-----		-----	-----	-----		
	4	1.000	.977	.966		1.000	1.282	1.179		
	5	-----	-----	-----		-----	-----	-----		
	6	1.000	.979	.972		1.000	1.009	1.026		
	7	-----	-----	-----		-----	-----	-----		
T-75/epoxy		Undamaged	After loading to			Undamaged	After loading to			
			0.036 GPa (5.2 ksi)	0.299 GPa (43.4 ksi)	0.309 GPa (44.8 ksi)	0.376 GPa (54.6 ksi)		0.036 GPa (5.2 ksi)	0.299 GPa (43.4 ksi)	0.309 GPa (44.8 ksi)	0.376 GPa (54.6 ksi)
	1	1.000	1.016	1.015	1.070	1.095	1.000	1.069	1.000	0.633	0.911
	2	1.000	1.012	1.030	1.048	1.078	1.000	4.074	.809	2.043	2.168
	3	1.000	1.002	.991	1.023	.958	1.000	1.423	1.588	1.369	2.765
	4	1.000	1.009	1.015	1.064	1.070	1.000	.930	1.070	1.139	1.077
	5	1.000	1.003	.988	1.023	.985	1.000	.820	1.372	.958	1.164
	6	1.000	1.007	1.007	1.061	1.057	1.000	1.000	1.605	.986	.986
	7	1.000	1.008	1.008	1.062	-----	1.000	.956	1.182	.960	-----

TABLE IV. - FREE VIBRATION FREQUENCIES OF UNDAMAGED AND DAMAGED COMPOSITES

Composite	Frequency order	Frequency, Hz								
		Experimental				Analytical				
		1	2	3	4	5	6	7	8	9
E-glass/epoxy		Undamaged	After loading to			Undamaged, no shear coupling	Undamaged, with shear coupling	Partial damage with shear coupling[a]	All elements damaged[b]	Slotted[c]
			0.193 GPa (28.2 ksi)	0.333 GPa (48.3 ksi)						
	1	830.1	781.2	781.2		815.3	813.8	803.9	738.2	802.4
	2	2246.1	2197.3	2246.1		2264.3	2259.8	2231.6	2051.0	2259.4
	3	------	------	------		2432.4	2427.5	2399.7	2187.6	2404.5
	4	4296.9	4199.2	4150.0		4469.4	4460.0	4376.6	4049.7	4427.4
	5	-----	------	------		4990.3	4980.1	4923.5	4490.0	4982.4
	6	7080	6933.6	6884.8		7426.8	7410.3	7374.5	6730.4	7407.2
T-75/epoxy		Undamaged	After loading to			Undamaged, with shear coupling	Partial damage with shear coupling	All elements damaged	Slotted	
			0.036 GPa (5.2 ksi)	0.299 GPa (43.4 ksi)	0.309 GPa (44.8 ksi)	no shear coupling				
	1	1035.1	1051.7	1060.9	1108.0	------	------	------	------	
	2	------	------	------	------	1395.9	1385.9	1366.4	1241.2	1368.9
	3	2877.9	2912.4	2962.9	3015.6	------	------	------	------	------
	4	4082.6	4092.4	4046.2	4177.1	3940.2	3907.0	3852.8	3501.8	3906.6
	5	5643.7	5692.3	5730.5	6002.4	5490.6	5453.9	5385.7	4879.8	5399.3
	6	8099.6	8124.2	8000.9	8283.9	7887.4	7819.4	7661.4	7008.6	7763.3
	7	9254.5	9316.8	9317.2	9814.6	------	------	------	------	------
	8	------	------	------	------	11181.6	11099.6	10962.0	9933.4	11104.7
	9	13550	13658	13660	14295	13252.5	13148.9	13064.0	11776.4	13134.8

[a]Moduli input for elements 57-64, 121-128, and 193-200 based on 0.2 void volume fraction.
[b]Moduli input for all elements based on 0.2 void volume fraction.
[c]Slot represented by removal of elements 124 and 125.

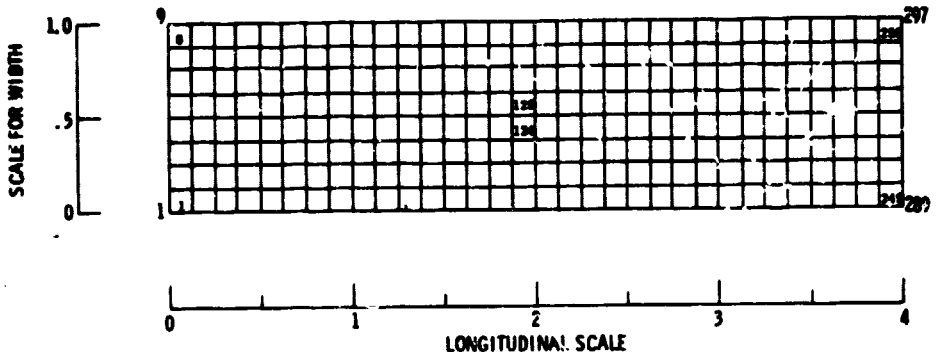

Figure 1. - NASTRAN model for composite specimens with defects (297 nodes, 256 elements, 1485 degrees of freedom (DOF)).

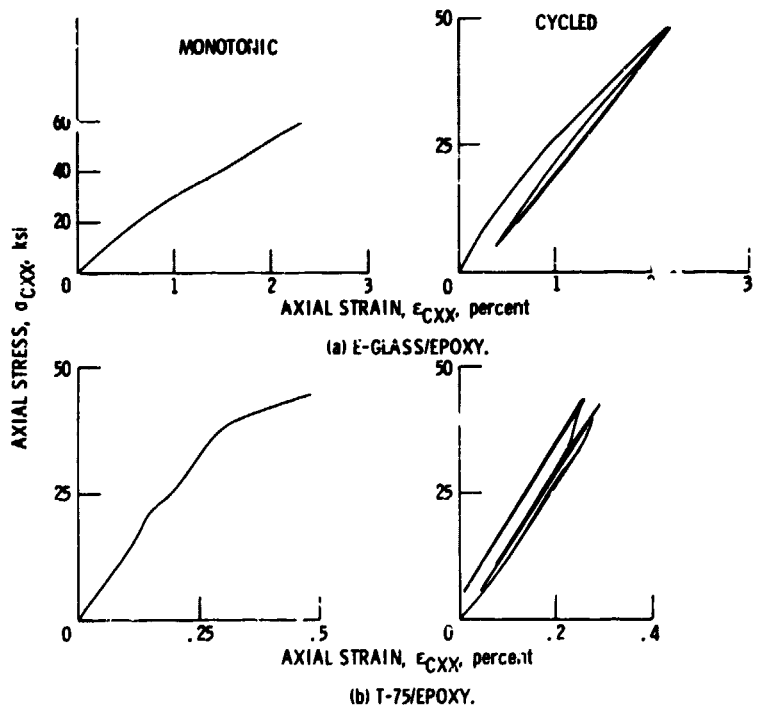

Figure 2. - Computer plotted stress-strain curves through experimental data (1 ksi = 6.8947 MPa).

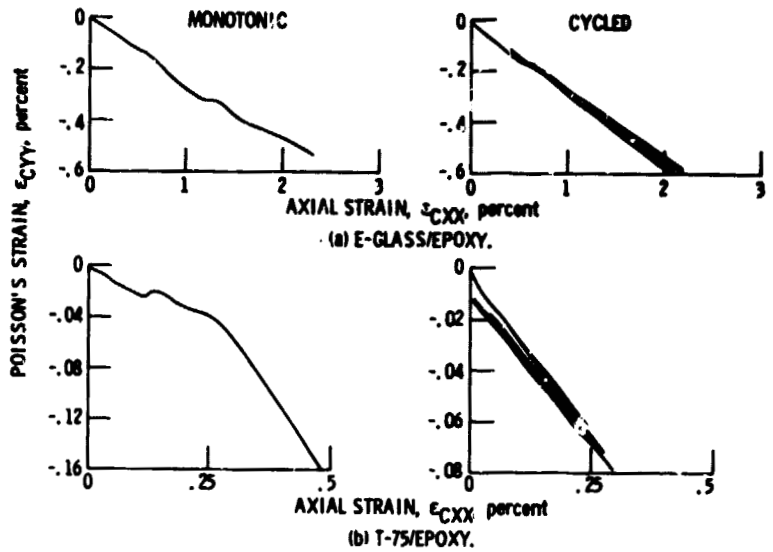

Figure 3. - Computer plotted transverse (Poisson) strain curves through experimental data.

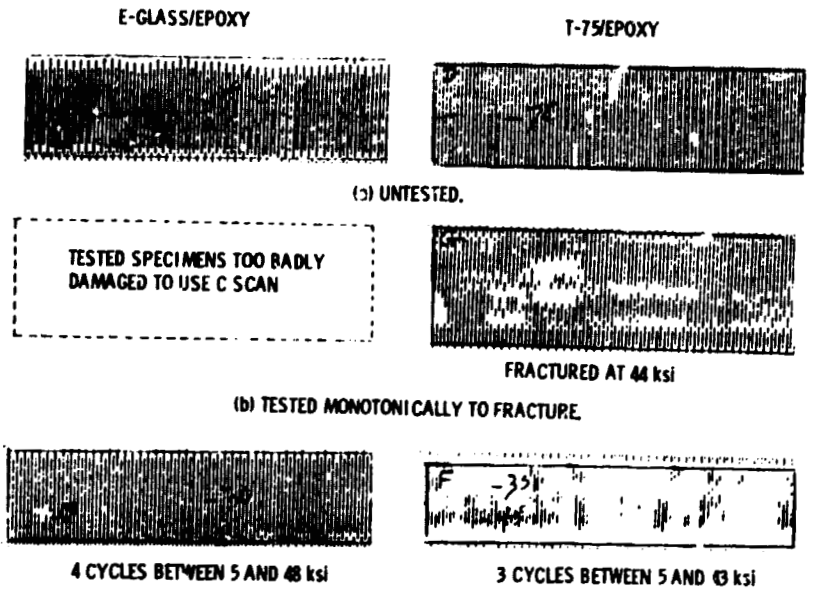

Figure 4. - C - Scans of untested composites and of tested specimens (1 ksi = 6.8947 MPa).

(a) E-GLASS/EPOXY.

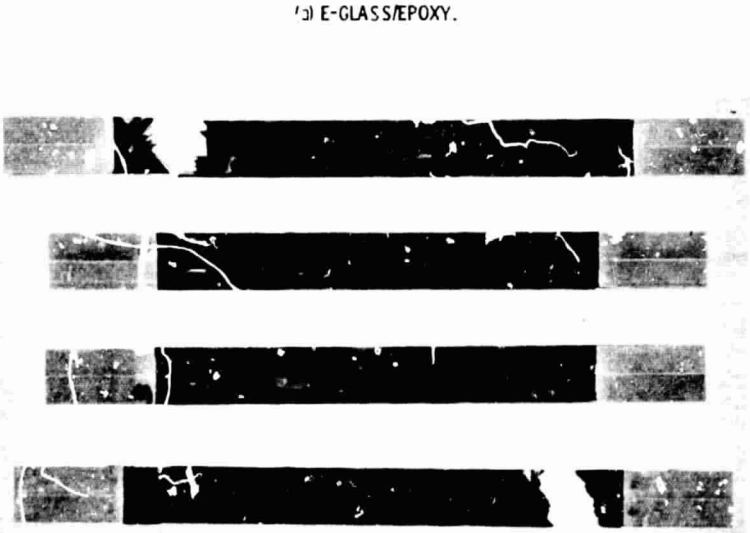

(b) T-75/EPOXY.

Figure 5. - Tested specimens.

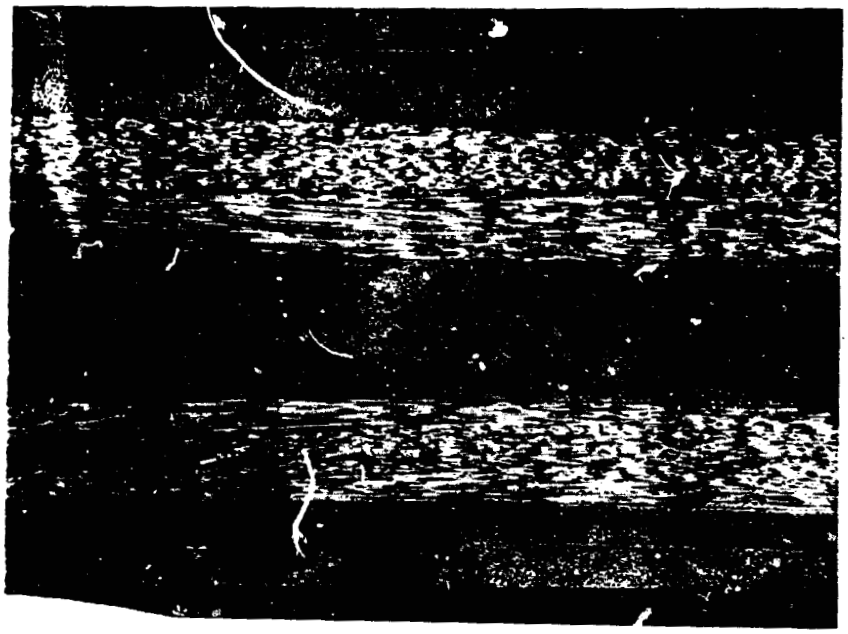

Figure 6. - Photomicrogrph showing transply cracks in $[\pm 45/90_2/0_2]_3$ Thornel 75/epoxy angleplied laminate.

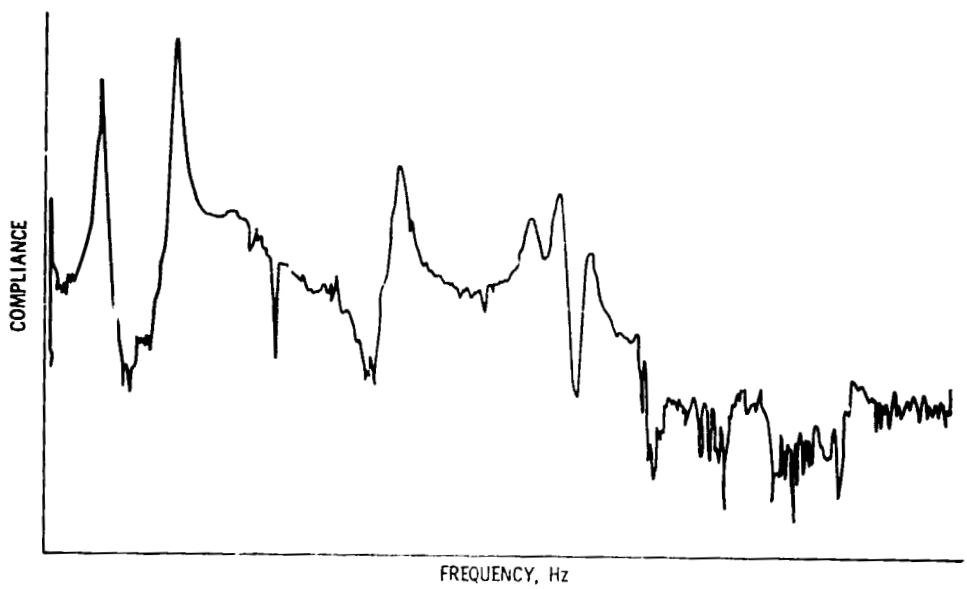

Figure 7. - Typical frequency response spectrum.

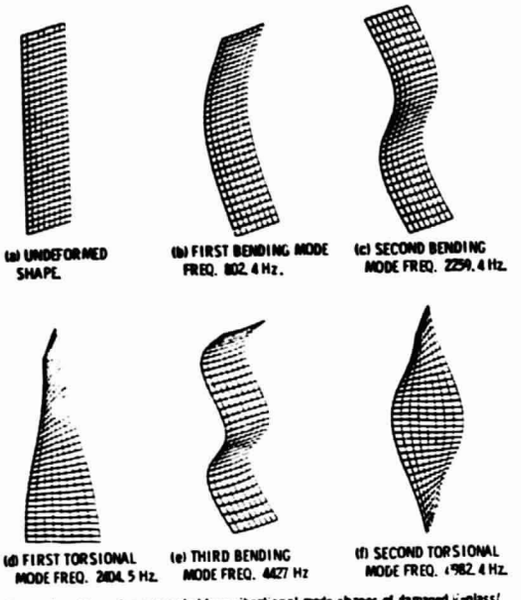

Figure 8. - Computer generated free vibrational mode shapes of damaged E-glass/epoxy specimen from angleplied composite $[\pm 45, 90_2, 0_2]_s$.

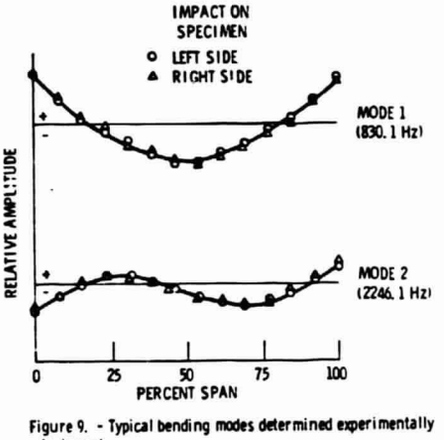

Figure 9. - Typical bending modes determined experimentally by impact.